CHINESE OPTICS LETTERS

Vol. 22, No. 5 | May 2024

High-precision alkali-atom density measurement and control methods using light absorption for dual-beam SERF magnetometers

Ziao Liu (刘子傲)[1,2], Jixi Lu (陆吉玺)[1,2,3*], Zhaohui Hu (胡朝晖)[1,2,3**], Xiaoyu Li (李晓昱)[1,2], Yifan Yan (闫一凡)[1,2,4], Di Zhan (詹 迪)[1,2], and Jianli Li (李建利)[1,2]

[1] Key Laboratory of Ultra-Weak Magnetic Field Measurement Technology, Ministry of Education, School of Instrumentation and Optoelectronic Engineering, Beihang University, Beijing 100191, China

[2] Zhejiang Provincial Key Laboratory of Ultra-Weak Magnetic-Field Space and Applied Technology, Hangzhou Innovation Institute, Beihang University, Hangzhou 310051, China

[3] Hefei National Laboratory, Hefei 230088, China

[4] Shen Yuan Honors College, Beihang University, Beijing 100191, China

*Corresponding author: lujixi@buaa.edu.cn

**Corresponding author: huzh@buaa.edu.cn

Received September 26, 2023 | Accepted January 15, 2024 | Posted Online May 14, 2024

The alkali-atom density measurement method based on light absorption is highly suitable for a spin-exchange relaxation-free (SERF) atomic magnetometer because of its high-precision measurement and complete nonmagnetic interference. In this study, the optical rotation angle detection system based on polarization balance detection is utilized to realize the alkali-atom density real-time measurement without affecting magnetic field measurement. We discovered that there exists an optimal frequency detuning of the probe light, which offers the highest sensitivity in alkali-atom density measurement and the lowest susceptibility to temperature fluctuations in terms of the scale factor. In contrast to conventional light absorption measurements based on pump light, this method demonstrated a threefold improvement in alkali-atom density measurement sensitivity while remaining immune to ambient magnetic fields and incident light intensity fluctuations. Furthermore, we utilized this method to achieve closed-loop temperature control with an accuracy of 0.04°C.

Keywords: light absorption; temperature measurement and control; dual-beam SERF magnetometer.
DOI: 10.3788/COL202422.051201

1. Introduction

Atomic magnetometers utilize atomic Larmor precession to provide magnetic field information with ultrahigh sensitivity, making them valuable for a wide range of applications, including biological magnetic field measurements, zero-field magnetic resonance, and magnetic anomaly detection[1–4]. Among the various kinds of atomic magnetometers, the spin-exchange relaxation-free (SERF) magnetometer is the most sensitive sensor and can achieve fT to sub-fT-level sensitivity[5,6]. To perform measurements in the SERF regime, atomic magnetometers require a near-zero field environment and a high alkali-atom density (10^{13}–10^{14} cm^{-3})[7,8]. The magnitude and stability of the alkali-atom density are critical factors affecting performance[9]. Therefore, high-precision measurement and control of alkali-atom density are significant for SERF magnetometers.

To achieve highly precise control, the measurement methods for the alkali-atom density in SERF magnetometers typically rely on either resistive temperature sensors or absorption spectroscopy. For the former method, an empirical formula is popularly used to deduce the saturated alkali vapor from the surface temperature of the vapor cell, which is usually detected by resistive temperature sensors (e.g., platinum resistance)[10,11]. The measurement result obtained by this method can exhibit a deviation from the actual alkali-atom density in the vapor cell[12]. In addition, since the resistive sensor requires driving currents, temperature sensors can inevitably introduce magnetic field interference, which affects the performance of atomic magnetometers[13]. In contrast, the alkali-atom density measurement method based on absorption spectroscopy offers several advantages, including high precision and nonmagnetic properties. In addition, this method directly detects the alkali-metal atomic density instead of the surface temperature of the vapor cell. These characteristics make it an ideal choice for SERF magnetometers, especially miniaturized ones, which are most susceptible to magnetic fields introduced by temperature sensors

owing to their compact sizes. In previous studies, this method has been successfully used. Yin *et al.* analyzed the influence of modulated magnetic fields on the transmitted intensity and achieved temperature control in SERF magnetometers by detecting the transmitted pump light intensity[14]. Liu *et al.* measured and controlled atomic number density over a wide temperature range based on light absorption[15]. The influence of static and oscillating magnetic fields on atomic number density measurements was also analyzed. However, these studies focused on the single-beam SERF magnetometer, and the measurement precision of the proposed method was susceptible to ambient magnetic fields and incident light intensity. For a dual-beam pump-probe configuration atomic magnetometer, which has higher measurement sensitivity, a more accurate measurement method is desirable. Thus, some alkali-atom density measurement methods based on light absorption have been referenced. Ito *et al.* measured the densities of K and Rb in a co-magnetometer, but this method exhibited an obvious deviation from the theoretical calculation results[16]. Ma *et al.* proposed a precise method for determining alkali-metal density using the atomic spin-exchange relaxation rate in atomic magnetometers[12]. However, the measurement of the spin-exchange relaxation rate was time-consuming, which made this method unsuitable for alkali-metal density control. Besides, Liu *et al.* also achieved the detection of atomic density in a K-Rb-^{21}Ne co-magnetometer using optical heterodyne interferometry which requires a complex optical path structure[17]. In summary, although the above methods have been successfully utilized to accurately measure alkali-atom density, these measurement methods are time-consuming or involve complex additional optical paths. Therefore, they are not well-suited for real-time control of alkali-atom density during magnetic field measurements.

Herein, we proposed a high-precision real-time method for alkali-atom density measurement and control based on light absorption for dual-beam SERF magnetometers. For this magnetometer configuration, the magnetic field was detected by measuring the optical rotation angle generated by the probe light passing through the vapor cell, which was measured using a balanced polarimetry technique. In this study, we utilized the sum of the two channels of the balanced polarimetry detector and the incident light intensity to obtain the linearly polarized light transmittance, thereby enabling the measurement of the alkali-metal density. Furthermore, we analyzed the influence of light-frequency detuning on temperature measurement sensitivity and discovered that there is an optimal value that maximizes the measurement sensitivity to alkali-metal density changes. Compared to conventional measurement methods based on pump light absorption, this study demonstrated a threefold improvement in alkali-atom density measurement sensitivity without requiring additional devices. Moreover, it offers the advantage of being immune to ambient magnetic fields and incident light intensity. Based on the above method, we further realized closed-loop temperature control with an accuracy of 0.04°C.

2. Methods

For SERF magnetometers, the atomic spin dynamics can be described by the Bloch equation[18,19],

$$\frac{\mathrm{d}\boldsymbol{P}}{\mathrm{d}t}=\frac{1}{q(P)}[\gamma_e\boldsymbol{B}\times\boldsymbol{P}+R_{\mathrm{op}}(s\hat{z}-\boldsymbol{P})-R_{\mathrm{rel}}\boldsymbol{P}], \tag{1}$$

where $\boldsymbol{P}$ is the electron polarization vector, $q(P)$ is the slowing-down factor, which depends on the spin polarization, $P=|\boldsymbol{P}|$, γ_e is the electron gyromagnetic ratio, $\boldsymbol{B}$ is the magnetic field vector, R_{op} is the pumping rate, s is the photon polarization (for circularly polarized light $s=1$; for linearly polarized light $s=0$), $\hat{z}$ is the unit vector along the pump beam, and R_{rel} is the spin relaxation rate. For a dual-beam pump-probe configuration magnetometer, the response to the magnetic field can be reflected by the optical rotation angle[20], whose simplified structure diagram is shown in Fig. 1. Assuming that the probe beam is along the x axis, the optical rotation angle of the linearly polarized probe light near the alkali-metal D1 transition is given by[20]

$$\theta=-\frac{1}{2}lr_e ncf_{\mathrm{D1}}\frac{\nu-\nu_0}{(\nu-\nu_0)^2+(\Gamma_L/2)^2}\frac{\gamma_e R_{\mathrm{op}}}{R_{\mathrm{tot}}^2+(\gamma_e B_y)^2}B_y, \tag{2}$$

where l is the optical path length, n is the alkali-atom density, r_e is the classical electron radius, c is the speed of light, f_{D1} is the oscillator strength of D1 transition, ν is the frequency of the incident laser, ν_0 is the resonance frequency of D1 line ($\nu-\nu_0=\Delta\nu$ is the frequency detuning), Γ_L is the pressure-broadened optical linewidth, $R_{\mathrm{tot}}=R_{\mathrm{op}}+R_{\mathrm{rel}}$ is the total spin-relaxation rate, and B_y is the measured magnetic field.

As shown in Fig. 1, the probe light intensity is measured using three photodetectors. Assuming that I_1 is the light intensity detected by PD1, I_2 is the light intensity detected by PD2, I_{in} is the incident light intensity detected by PD3, and I_{out} is the light intensity transmitted through the vapor cell, which can be obtained by summing I_1 and I_2. The differential signals of I_1 and I_2 are used to detect the magnetic field information reflected in the optical rotation angle, as $I_2-I_1=I_{\mathrm{out}}\sin(2\theta)$. As the detected optical rotation angle is usually very small, $\theta\ll 1$, the above equation can be rewritten as $I_2-I_1\approx 2I_2\theta$. In addition, the sum of I_1 and I_2 divided by I_3 is the transmittance of the probe beam passing through the vapor cell, which can be used to measure the alkali-atom density without altering the original measurement setup.

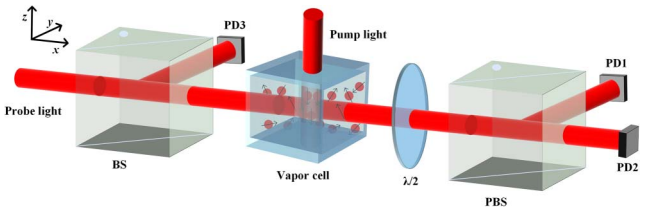

Fig. 1. Schematic of the dual-beam magnetometer. λ/2, half-wave plate; BS, beam splitter; PBS, polarization beam splitter; PD, photodetector.

When linearly polarized light passes through the vapor cell, the plane of polarization of linearly polarized light is rotated by an angle θ and the transmittance of the linearly polarized light is a function of the alkali-atom density, which can be described by[21]

$$\frac{I_{\text{out}}}{I_{\text{in}}} = \exp[-n\sigma(\nu)l], \tag{3}$$

where $\sigma(\nu)$ is the photon absorption cross section, which can be expressed as[14]

$$\sigma(\nu) = r_e c f_{\text{D1}} \frac{\Gamma_L/2}{\Delta\nu^2 + (\Gamma_L/2)^2}. \tag{4}$$

For the pump light, the incident light frequency is usually set to the atomic resonance center frequency of the D1 line, and the photon absorption cross section can be expressed as $\sigma(\nu_0) = 2r_e c f_{\text{D1}}/\Gamma_L$. In contrast to the pump light, the orthogonal probe light is typically detuned 100 GHz off-resonance from the center frequency of the D1 line to avoid being completely absorbed by the optically thick cell, which results in a weak detection signal[22,23].

To reflect the sensitivity of the transmittance to the unit alkali-metal density change in this measurement method, we calculate the partial derivative of the transmittance with respect to alkali-metal density, whose absolute value is defined as the measurement sensitivity,

$$S_{\text{probe}}(n) = |-\sigma(\nu)l \exp[-n\sigma(\nu)l]|. \tag{5}$$

Combining Eqs. (4) and (5), it can be seen that if we assume vapor cell parameters in the experiment to be fixed, the measurement sensitivity of alkali-atom density will be determined by the light-frequency detuning $\Delta\nu$ of the probe beam. To achieve optimal measurement sensitivity, we calculated the partial derivative of the measurement sensitivity with respect to light-frequency detuning $\Delta\nu$, as shown in Eq. (6),

$$\frac{\mathrm{d}S_{\text{probe}}(n)}{\mathrm{d}\Delta\nu} = \frac{K_1\left[1 - K_2 \frac{\Delta\nu^2 + (\Gamma_L/2)^2}{\Gamma_L/2}\right]}{(\Gamma_L^2 + 4\Delta\nu^2)^3}, \tag{6}$$

where $K_1 = 16cf_{\text{D1}}lr_e\Gamma_L\Delta\nu \exp[-2ncf_{\text{D1}}lr_e\Gamma_L/(\Gamma_L^2 + 4\Delta\nu^2)]$ and $K_2 = 1/nlcf_{\text{D1}}r_e$. When the above equation is equal to zero, the sensitivity reaches its maximum value, indicating that the light frequency detuning $\Delta\nu$ reaches its optimal value:

$$\Delta\nu_{\text{op}}^2 = \frac{ncf_{\text{D1}}lr_e\Gamma_L}{2} - \left(\frac{\Gamma_L}{2}\right)^2. \tag{7}$$

Combined with Eq. (4), the optical depth [$\text{OD} = n\sigma(\nu)l$] can be determined based on the optimal light frequency detuning $\Delta\nu_{\text{op}}$, and the result shows that it is 1 ($\text{OD} = 1$). Based on previous studies, we found that in dual-beam SERF magnetometers, setting the optical depth to 1 can also minimize the susceptibility of the magnetic field measurement to fluctuations in the alkali-metal density[24]. Therefore, the proposed optimization method for light frequency detuning $\Delta\nu$ not only maximizes the measurement sensitivity of alkali-atom density but also effectively improves the performance of dual-beam SERF magnetometers.

To demonstrate the superiority of this method in the measurement sensitivity, we conducted a comparative analysis with an alkali-atom density measurement method based on circularly polarized pump light absorption. The propagation of circularly polarized pump light in the vapor cell can be described as[18]

$$\frac{I_z}{I_0} = \frac{h\nu_0}{\sigma(\nu_0)I_0} R_{\text{rel}} W\left\{\frac{\sigma(\nu_0)I_0}{h\nu_0 R_{\text{rel}}} \exp\left[\frac{\sigma(\nu_0)I_0}{h\nu_0 R_{\text{rel}}} - n\sigma(\nu_0)l\right]\right\} \tag{8}$$

where h is Planck's constant. The measurement sensitivity of this method can be defined in the same way as Eq. (5), which has the following form:

$$S_{\text{pump}}(n) = \left| -\frac{\text{OD}}{nK_3\left\{1 + \frac{1}{W[K_3 \exp(K_3 - \text{OD})]}\right\}}\right|, \tag{9}$$

where $K_3 = \sigma(\nu_0)I_0/h\nu_0 R_{\text{rel}}$ is a parameter related to the incident pump light intensity I_0 and the spin relaxation rate R_{rel}. Assuming the light frequency detuning $\Delta\nu$ of probe light is set as the above optimal value, by combining Eqs. (5) and (9), we can compare the sensitivities of the two aforementioned methods using

$$\frac{S_{\text{probe}}(n)}{S_{\text{pump}}(n)} = \frac{K_3}{\text{OD}\exp(1)}\left\{1 + \frac{1}{W[K_3 \exp(K_3 - \text{OD})]}\right\}. \tag{10}$$

When the vapor cell parameters in the experiment are fixed, the indeterminate terms K_3 and OD in Eq. (10) are primarily influenced by pump light intensity and temperature, respectively. Thus, we conducted a fitting experiment for Eq. (10) at different pump light intensities and temperatures, as described below. In addition, by comparing Eqs. (3) and (8), we can observe that the transmittance of linearly polarized light through the vapor cell is unaffected by the incident light intensity and the relaxation rate R_{rel}, which is greatly affected by ambient magnetic fields. Thus, the proposed method is more immune to environmental noise than the conventional method.

3. Experimental Setup

The experimental setup for the SERF magnetometer is shown in Fig. 2. We used a cubic glass cell with inner dimensions of 8 mm × 8 mm × 8 mm. The vapor cell contained a droplet of ^{87}Rb and was filled with approximately 2100 Torr of N_2 as buffer and quenching gas. Two flexible heating films were placed in parallel to heat the vapor cell inside an oven powered by an AC current at 500 kHz[25]. A four-layer cylindrical μ-metal magnetic shield was employed to isolate the external magnetic field, and a triaxial coil was mounted to compensate for the residual magnetic field.

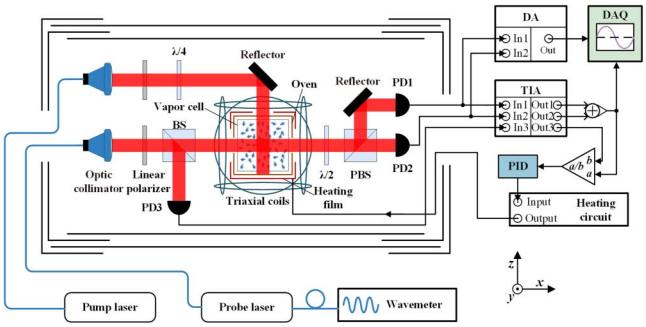

Fig. 2. Experimental setup of the dual-beam SERF magnetometer for alkali-atom density measurement and control based on light absorption. DA, differential amplifier; DAQ, data acquisition; TIA, transimpedance amplifier; BS, beam splitter; PBS, polarization beam splitter; PD, photodetector; $\lambda/2$, half-wave plate; $\lambda/4$, quarter-wave plate.

The pump light tuned to the ^{87}Rb D1 resonance line was generated by an external-cavity diode laser (Toptica DLpro), and the probe light was detuned to approximately 100 GHz from the ^{87}Rb D1 resonance line generated by a distributed feedback (DFB) laser. Both were transmitted to the OPM via a polarization-maintaining fiber (PMF). During the experiment, the wavelength of the probe beam was monitored using a wavemeter (HighFinesse WS-6). A beam splitter was placed in front of the vapor, which enabled photodetector PD3 to detect the incident light intensity of the vapor cell. After passing through the vapor cell, the probe light was geometrically split using a balanced polarimetry beam splitter and detected using PD1 and PD2. The differential and common signals of the two PDs were used to detect the optical rotation angle and transmitted light intensity, respectively.

In our experiments, we first verified the accuracy of the proposed method for measuring the alkali-atom density. Subsequently, the influence of light-frequency detuning on the measurement sensitivity was analyzed. In addition, a comparative analysis of the alkali-atom density measurement method based on pump light absorption was conducted to demonstrate the superior measurement sensitivity of the proposed method. Finally, we utilized this method to achieve closed-loop temperature control inside the vapor cell using a proportional integral and derivative (PID) controller.

4. Results and Discussions

We conducted a comparison experiment between the measured and theoretically calculated Rb atom densities at different temperatures, as shown in Fig. 3. The vapor cell temperature was heated from 50°C to 160°C. The incident light intensity was set to 30 mW/cm^2 and recorded using PD3. The transmitted light intensity was proportional to the sum of the output signals of PD1 and PD2. Hence, the actual measurement values were calculated based on light transmittance at different temperature points through Eq. (3). The theoretical values of the alkali-atom density at different temperatures were obtained using the

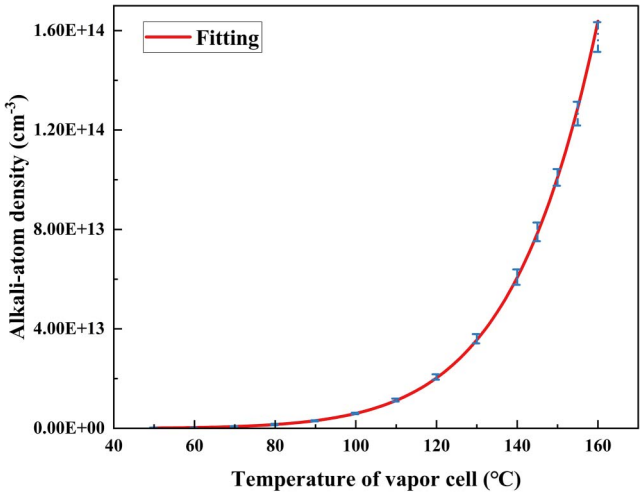

Fig. 3. Comparison between measured values and theoretical values from saturated vapor pressure formula.

saturated vapor pressure formula, which can be described by Eq. (11),

$$n = \frac{1}{T} 10^{21.866 + A - B/T}, \tag{11}$$

where T is the temperature in Kelvin. A and B are constants determined by the alkali metal. For the ^{87}Rb, $A = 4.312$ and $B = 4040$[26].

The comparison results demonstrated good agreement between the proposed alkali-atom density measurement method and theoretical values. The measurement standard deviation of this method gradually increased with temperature, which is caused by the exponential relationship between the alkali-atom density and temperature. When the temperature of the vapor cell increased to 160°C, the density measurement exhibited a standard deviation of 3.8%, while the temperature measurement deviation remained below 1°C.

The optimal light frequency for this method was determined as follows. We measured the sensitivity of alkali-atom density measurement at 150°C with different light frequencies, which is a common operating temperature for Rb SERF magnetometers. And the sensitivity was measured as the alteration in transmittance resulting from a 10^{13} cm^{-3} shift in alkali-atom density. Following the saturated vapor pressure formula, a rise in vapor cell temperature from 149°C to 151°C leads to an increase of 10^{13} cm^{-3} in alkali-atom density. Therefore, the sensitivity at 150°C defined by Eq. (5) is measured as the difference in transmittance between 149°C and 151°C. The light-frequency detuning $\Delta\nu$ was varied from 30 to 120 GHz. Figure 4 shows the measurement and fitting results of Eq. (5).

The experimental results were in good agreement with the expected results. When the light-frequency detuning $\Delta\nu$ was set to 80 GHz (OD $\approx$ 1), the sensitivity of the alkali-atom density measurement reached its maximum value. The sensitivity variation trend with light-frequency detuning $\Delta\nu$ was similar to that

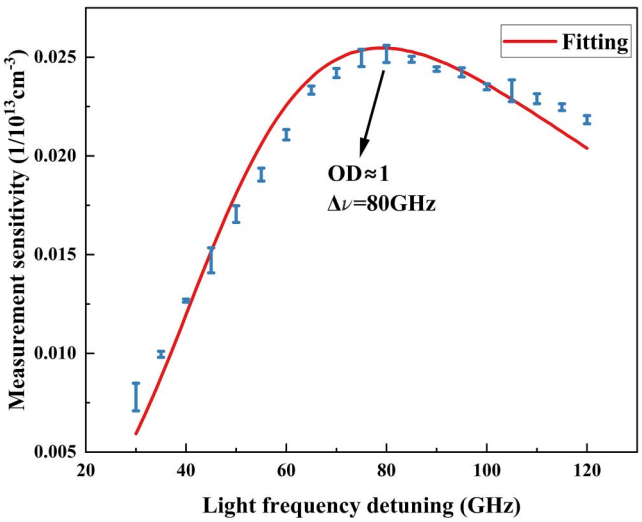

Fig. 4. Relationship between the measurement sensitivity of alkali-atom density and the light-frequency detuning $\Delta\nu$.

of the fitting curve. This optimal light-frequency detuning offered the highest sensitivity in alkali-atom density measurement and the lowest susceptibility to temperature fluctuations in magnetic field measurements.

To demonstrate the superior sensitivity of this method, it was compared with a measurement method based on pump light absorption at different temperatures and pump light intensities by fitting Eq. (10). The temperature was varied from 140°C to 160°C, and the light intensity of the incident pump light was varied from 20 to 70 mW/cm^{-2}. The sensitivity comparison of the proposed method to the conventional method based on pump light is shown in Fig. 5.

We can observe that the proposed method demonstrated a significant improvement in measurement sensitivity, ranging from 1.2 to 8.2 times, within the specified range of cell

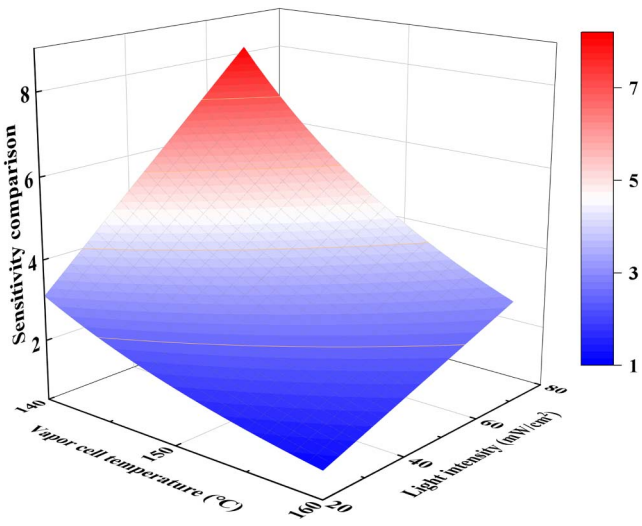

Fig. 5. Fitting result of the comparative experiments at different temperatures and light intensities.

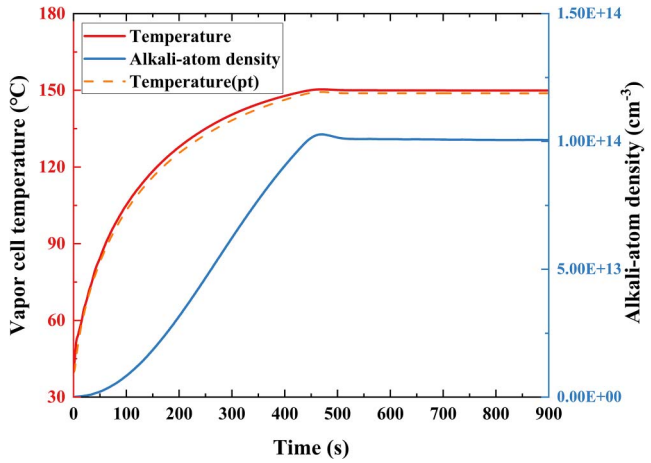

Fig. 6. Variations of the alkali-atom density and temperature over time.

temperature and light intensity. The main reason is that the incident pump light is not set to the optimal value for alkali-atom density measurement, which will influence the performance of magnetometers. Actually, the selection of the pump light intensity in practical application is usually based on the response strength of magnetometers for magnetic fields rather than considering the measurement sensitivity of the alkali-atom density. For the operating conditions in this experimental setup, at 150°C and 30 mW/cm^2, this method offers about a threefold improvement in sensitivity.

Based on the above alkali-atom density measurement method, we further applied a PID controller. In this experiment, we used a temperature-control program encoded in LabVIEW to drive the electric heater. The target temperature is set as 150°C, which is calculated from the measured alkali-atom density. We also recorded the surface temperature of the vapor cell using a nonmagnetic platinum resistance (pt1000). The variations in temperature and alkali-atom density under closed-loop control are shown in Fig. 6.

The vapor cell temperature reaches 150°C at 500 s after heating and maintains this temperature. After the vapor cell temperature is stabilized, the mean of temperature in 400 s is 149.95°C, and a standard deviation of 0.04°C is calculated. The maximum temperature deviation is 0.07°C and the maximum fluctuation of the alkali-atom density is approximately 0.24%. Hence, this alkali-atom density control method based on light absorption was verified to meet the operating requirements of the SERF magnetometers. We also discovered that the temperature measurement result of the platinum resistance is 148.8°C when temperature remains constant. The main reason for the measurement deviation was the disparity between the surface temperature and actual temperatures inside the vapor cell.

5. Conclusion

In this study, a high-precision alkali-atom density measurement method based on light absorption was developed for SERF magnetometers. An optical rotation angle detection system based on

a balanced polarimetry technique was used to measure the alkali-atom density without altering the original measurement setup. Based on the analysis of this method, we also found that there was an optimal light-frequency detuning for this method that led to the highest sensitivity in alkali-atom density measurements and the lowest susceptibility to temperature fluctuations in magnetic measurements. Compared to the conventional alkali-atom density measurement method based on pump light absorption, this method exhibited a remarkable threefold improvement in the alkali-atom density measurement sensitivity at the setting point. Furthermore, it was immune to variations in incident light intensity and ambient magnetic fields. Based on the proposed method, we further implemented closed-loop temperature control with an accuracy of 0.04°C. The maximum fluctuation in the alkali-atom density was limited to 0.24%. Thus, this study provides a useful alkali-atom density measurement method for SERF magnetometers and facilitates the application of alkali-atom density control in other types of miniaturized atomic sensors using balanced polarimetry technology.

References

1. E. Boto, N. Holmes, J. Leggett, *et al.*, "Moving magnetoencephalography towards real-world applications with a wearable system," Nature **555**, 657 (2018).
2. G. Roberts, N. Holmes, N. Alexander, *et al.*, "Towards OPM-MEG in a virtual reality environment," NeuroImage **199**, 408 (2019).
3. T. Theis, P. Ganssle, G. Kervern, *et al.*, "Parahydrogen-enhanced zero-field nuclear magnetic resonance," Nat. Phys. **7**, 571 (2011).
4. S. J. Seltzer and M. V. Romalis, "Unshielded three-axis vector operation of a spin-exchange-relaxation-free atomic magnetometer," Appl. Phys. Lett. **85**, 4804 (2004).
5. T. Karaulanov, I. Savukov, and Y. J. Kim, "Spin-exchange relaxation-free magnetometer with nearly parallel pump and probe beams," Meas. Sci. Technol. **27**, 055002 (2016).
6. Y. Chen, W. Quan, S. Zou, *et al.*, "Spin exchange broadening of magnetic resonance lines in a high-sensitivity rotating K-Rb-^{21}Ne co-magnetometer," Sci. Rep. **6**, 36547 (2016).
7. H. B. Dang, A. C. Maloof, and M. V. Romalis, "Ultrahigh sensitivity magnetic field and magnetization measurements with an atomic magnetometer," Appl. Phys. Lett. **97**, 151110 (2010).
8. J. Lu, S. Wang, F. Lu, *et al.*, "Hybrid optimal design of square highly uniform magnetic field coils," IEEE Trans. Ind. Electron. **70**, 4236 (2023).
9. V. Shah and M. V. Romalis, "Spin-exchange relaxation-free magnetometry using elliptically polarized light," Phys. Rev. A **80**, 013416 (2009).
10. J. Zhao, M. Ding, J. Lu, *et al.*, "Determination of spin polarization in spin-exchange relaxation-free atomic magnetometer using transient response," IEEE Trans. Instrum. Meas. **69**, 845 (2020).
11. S. Pradhan and R. Behera, "Characterization of polarimetric based three axis atomic magnetometer," Sens. Actuators A **290**, 48 (2019).
12. Y. Ma, Y. Chen, L. Zhao, *et al.*, "Accurate determination of alkali atom density based on zero-field magnetic resonance in a single-beam spin-exchange relaxation-free atomic magnetometer," Meas. Sci. Technol. **33**, 105003 (2022).
13. J. Lu, W. Quan, M. Ding, *et al.*, "Suppression of light shift for high-density alkali-metal atomic magnetometer," IEEE Sens. J. **19**, 492 (2019).
14. Y. Yin, B. Zhou, K. Yin, *et al.*, "The influence of temperature and modulated magnetic field on the transmission intensity of atomic magnetometer," J. Phys. D **54**, 485001 (2021).
15. Z. Liu, J. Lu, Y. Yan, *et al.*, "*In-situ* measurement and close-loop control of atomic number density in an optically pumped magnetometer based on light absorption," Meas. Sci. Technol. **34**, 085108 (2023).
16. Y. Ito, H. Ohnishi, K. Kamada, *et al.*, "Development of an optically pumped atomic magnetometer using a K-Rb hybrid cell and its application to magnetocardiography," AIP Adv. **2**, 032127 (2012).
17. S. Liu, Z. Wang, and Y. Zhai, "*In-situ* detection for atomic density in the K-Rb-^{21}Ne Co-magnetometer via an optical heterodyne interferometry," Photonics **10**, 1091 (2023).
18. S. J. Seltzer, *Developments in Alkali-Metal Atomic Magnetometry* (Princeton University, 2008).
19. Y. Yan, J. Lu, S. Zhang, *et al.*, "Three-axis closed-loop optically pumped magnetometer operated in the SERF regime," Opt. Express **30**, 18300 (2022).
20. M. P. Ledbetter, I. M. Savukov, V. M. Acosta, *et al.*, "Spin-exchange-relaxation-free magnetometry with Cs vapor," Phys. Rev. A **77**, 033408 (2008).
21. Z. Ding, J. Yuan, Z. Wang, *et al.*, "Optically pumped rubidium atomic magnetometer with elliptically polarized light," Optik **127**, 5270 (2016).
22. S. J. Smullin, I. M. Savukov, G. Vasilakis, *et al.*, "Low-noise high-density alkali-metal scalar magnetometer," Phys. Rev. A **80**, 033420 (2009).
23. X. Zhang, J. Qin, Y. Wang, *et al.*, "A fast identification on the spin-exchange relaxation-free regime of atomic magnetometer exploiting measurement on gyromagnetic ratio," IEEE Trans. Instrum. Meas. **68**, 1157 (2019).
24. J. Lu, Z. Qian, J. Fang, *et al.*, "Suppression of vapor cell temperature error for spin-exchange-relaxation-free magnetometer," Rev. Sci. Instrum. **86**, 083103 (2015).
25. J. Lu, C. Lu, S. Wang, *et al.*, "Optimized electric heater configuration design with magnetic-field self-suppression using genetic algorithm," Sens. Actuators A **344**, 113758 (2022).
26. C. B. Alcock, V. P. Itkin, and M. K. Horrigan, "Vapour pressure equations for the metallic elements: 298–2500 K," Can. Metall. Q. **23**, 309 (1984).